Med Biol Eng Comput (2016) 54:1903–1920
DOI 10.1007/s11517-016-1481-1

ORIGINAL ARTICLE

Robust segmentation and intelligent decision system for cerebrovascular disease

Asmatullah Chaudhry[1] · Mehdi Hassan[2,3] · Asifullah Khan[2]

Received: 17 June 2015 / Accepted: 28 February 2016 / Published online: 7 April 2016

Abstract Segmentation and classification of low-quality and noisy ultrasound images is challenging task. In this paper, a new approach is proposed for robust segmentation and classification of carotid artery ultrasound images and consequently, detecting cerebrovascular disease. The proposed technique consists of two phases, in first phase; it refines the class labels selected by user using expectation maximization algorithm. Genetic algorithm is then employed to select discriminative features based on moments of gray-level histogram. The selected features and refined targets are fed as input to neuro-fuzzy classifier for performing segmentation. Finally, intima-media thickness values are measured from segmented images to segregate the normal and abnormal subjects. In second phase, an intelligent decision-making system based on support vector machine is developed to utilize the intima-media thickness values for detecting cerebrovascular disease. The proposed robust segmentation and classification technique for ultrasound images (RSC-US) has been tested on a dataset of 300 real carotid artery ultrasound images and yields accuracy, *F*-measure, and MCC scores of 98.84, 0.988, 0.9767 %, respectively, using jackknife test. The segmentation and classification performance of the proposed (RSC-US) has been also tested at several noise levels and may be used as secondary observation.

✉ Mehdi Hassan
mhassan@aumc.edu.pk; mehdi.hassan5@gmail.com

[1] DMIS, PAEC-HQ, Islamabad, Pakistan

[2] Pattern Recognition Lab, PIEAS, P.O. Nilore, Islamabad 45650, Pakistan

[3] Air University, PAF Complex, Sector E-9, Islamabad, Pakistan

Keywords Carotid artery image segmentation · Fuzzy inference system · Expectation maximization · Intima-media thickness · Support vector machine · Cerebrovascular accident

1 Introduction

Cerebrovascular disease is the fourth major cause of deaths, with a number of 129,476 deaths in USA only, in the year 2010 [33]. The *ischemic* and the *hemorrhagic* strokes are the two common types of cerebrovascular accidents. The ischemic stroke occurs due to blockage of carotid artery by plaque. On the other side, the hemorrhagic stroke occurs due to rupture of blood vessels in brain. Early plaque detection may prevent such strokes.

Carotid angiography utilizing X-ray imaging is considered as a standard technique for carotid artery plaque detection. The plaque is formed due to presence of fatty materials in carotid artery. Whereby, plaque formation may fully or partially block the oxygenated blood flow to the brain and thus resulting in a brain stroke. Moreover, if the plaque ruptures, small components may drift into the brain, and it may cause a cerebrovascular accident. In this case, an early information and thus detection of plaque can prevent such adverse effects.

Carotid angiography is an invasive nature and associated with various drawbacks including an injection of X-ray dye. Further, this process is process risky, uncomfortable, includes allergic reactions, and may result in kidney failure and radiation hazards. On the other hand, noninvasive nature of ultrasound imaging is a popular tool for plaque assessment in common carotid artery. However, ultrasound images have some inherent limitations such as speckle noise, low quality, and other artifacts. Consequently, it needs significant efforts from radiologists to examine plaque in carotid artery. Moreover, manual extraction of carotid artery contour is a tedious job that may vary from expert to expert and may overburden the radiologists. Hence, computer-aided diagnosis (CAD) system is essential to automatically analyze the carotid artery ultrasound images. Further, it can also serve as a secondary observer and may help radiologists to assess the seriousness of plaque into carotid artery [19, 20].

Imaging techniques such as, magnetic resonance imaging (MRI), computed tomography (CT), and ultrasound imaging, allow acquisition of images in a noninvasive way. Experts can diagnose disease by analyzing such images; however, it needs considerable effort from radiologists. In this connection, CAD is a highly desirable tool to help radiologists in analyzing medical images and diagnosing the disease. The CAD systems usually segment medical images and further processing is carried out on these segmented images. Image segmentation has a significant role in various medical image analysis tasks such as quantification of tissue volume [41], treatment planning [40], anatomical structure study [38], diagnosis [8], and computer-aided surgery [4]. In literature, many techniques have been reported to segment medical images [6, 15, 21, 24, 25, 30], but none of them can coup simultaneously with all of the problems (noise, low-quality image etc.).

The efficacy of post-processing techniques in medical imaging highly depends upon the quality of segmentation. A slight change in segmentation results heavily affects the post-processing step and may produce harmful consequences in medical diagnosis. On the other hand, a small improvement in segmentation may contribute enormously to the post-processing steps. Hence, accurate segmentation has significant influence on computer based disease diagnosis. Nonetheless, medical images can suffer from degradations such as low resolution, noise, partial volume effect, and other artifacts. Due to these degradations, segmentation of medical image may produce misleading results. For instance, ultrasound images are generally affected by speckle noise, low resolution, and wave interferences. Keeping in view the above-mentioned problems, accurate and robust segmentation of ultrasound images is considered a challenging task.

Several medical image segmentation techniques have been reported in literature. Each and every technique has its own limitations. For example, Chung et al. [11] have reported a technique namely spatial fuzzy *c*-means (sFCM) for medical image segmentation. In their technique, the basic FCM framework is modified by exploiting pixel's spatial information. However, sFCM assigns same weight to each pixel in a subimage and thus produces non-homogenous clustering. Further, Chaudhry et al. [8] have reported modification in the sFCM technique and named their modified technique as spatial fuzzy *c*-means modified (sFCMM) technique. In SFCMM, weight of every pixel is based on its distance from central pixel and hence produces homogenous clustering. SFCMM works well at lower noise levels; however, it may not offer superior clustering at higher noise level. Alternatively, Li et al. [23] have reported a segmentation technique for medical imaging, which incorporates spatial fuzzy clustering with level set methods (sFCMLSM). They performed fuzzy clustering in association with partial differential equations, which are computationally expensive.

The ultimate purpose of carotid artery image segmentation is to segregate the arterial walls from background tissues. Deformable model-based carotid artery lumen extraction technique was reported by Mao et al. [29]. Similarly, Loizou et al. [26] have proposed an integrated segmentation scheme of carotid artery images. Their approach employs a snake-based model for segmentation. Snake and other deformable models need initializations from users, and inexperienced users may initialize the model improperly which can lead toward misleading results.

Hassan et al. [15] have proposed segmentation technique for carotid artery ultrasound images and have accomplished performance analysis using sFCMM and ensemble clustering. They have extracted three different types of features namely, MGH, 2-D continuous wavelet transform (2D-CWT), and gray-level co-occurrence matrix (GLCM). The discernment features were selected using GA. Their technique works well at lower noise level, but may not produce significant results at high intensity noise.

Abdel-Dayem et al. [1] have used watershed segmentation technique for carotid artery ultrasound image segmentation. However, watershed may sometimes result in over segmentation. Further, the selection of appropriate threshold at region merging stage is vital in this approach. Moreover, Kamel et al. [20] proposed fuzzy region growing based technique for carotid artery ultrasound images. However, their method is computationally expensive due to consideration of fuzzy map.

An interesting approach for carotid artery ultrasound image segmentation based on Hough transform has been reported in [14]. However, Hough transform-based techniques are suitable to detect lines and circles. Since, due to curvy nature of the carotid artery vessels, Hough transform may not perform well to segment carotid artery images. Further in [14], the reported technique scheme at 10 B (bright)-mode ultrasound images, but the evaluation was performed for small level stenosis, and additionally, the robustness of their approach was not gauged. On the other hand, Xu et al. [42] have reported a segmentation scheme for carotid artery ultrasound images based on Hough transform and dual-snake models. Accurate snake initialization is a challenging task and inappropriate initialization may produce misleading results. Further, Hough transform-based techniques may not work well, owing to the curvy nature of arterial walls. Further in [42], the robustness of the method has not been evaluated at noisy variants of the carotid artery ultrasound images.

Christodoulou et al. [10] have proposed a texture-based classification of carotid artery plaque. A total of 22 statistical and gray-level dependence matrix features have been extracted from given image. These features were further used for carotid plaque classification. Their technique is computationally expensive due to the use of a large-dimensional feature vector. Keeping in view this aspect, Rocha et al. [36] have proposed RANSAC and cubic spline-based segmentation technique. They have tested their technique by using 50 B (bright)-mode carotid artery images.

Segmentation of low-quality and noisy ultrasound images is challenging task. In this paper, we propose a new hybrid technique for segmentation and classification of carotid artery ultrasound images to detect plaque in carotid artery and thus apprise of any possible cerebrovascular accidents. For this purpose, a robust and accurate segmentation technique by exploiting the concepts of neuro-fuzzy, expectation maximization, and genetic algorithm has been proposed. SVM-based classification is then employed using a significant number of real carotid artery ultrasound images segmented by the proposed approach. It is a well-known fact that post-processing techniques highly depend upon segmentation accuracy. This implies that proper and correct segmentation has great impact on classification results. IMT value is mostly used as a feature in carotid artery disease classification, and if image has not been segmented correctly, this may result in incorrect IMT measurement. Consequently, it may lead to misclassification of the object at hand.

The proposed technique comprises three main stages. In the first phase, EM algorithm is applied for finding the accurate target of each class pixels. Further, MGH image feature extraction and selection, neuro-fuzzy classifier training and validation, and generation of FIS steps are performed. In the second phase, carotid artery ultrasound images are segmented by employing FIS generated from phase-I. Third phase of our proposed approach is measurement of the IMT values and classification of the segmented carotid artery images into abnormal or normal subjects. SVM classifier has then been employed to distinguish the abnormal subjects from normal ones.

Rest of the paper is organized as follows. Section 2 explains the proposed hybrid approach. Results and discussions are presented in Sect. 3. Finally, conclusions and future recommendations are drawn in Sect. 4.

The abbreviations used in this paper are listed in Table 1.

Table 1 Abbreviations used in the paper

GA	Genetic algorithm
NFC	Neuro-fuzzy classifier
IMT	Intima-media thickness
EM	Expectation maximization
MGH	Moments of gray-level histogram
SVM	Support vector machine
DBI	Davies–Bouldin index
AUC	Area under the curve
IMT	Intima-media thickness
RSC-US	Robust segmentation and classification of ultrasound images
sFCMM	Spatial fuzzy *c*-means modified
CAD	Computer-aided diagnosis

2 Methods

The principal objective of the proposed scheme is to accurately segment the carotid artery ultrasound images. IMT values have been measured from segmented images (using the proposed scheme) and subsequently, used for classification. Further, SVM classifier has been utilized to classify the proposed approach segmented images of dataset into abnormal or normal subjects.

Ultrasound images have many types of limitations such as, lower quality, presence of noise, and other artifacts. Further, due to high pixel correlation especially in ultrasound images, it is very difficult to identify the correct label for each pixel. For accurate and robust segmentation, it is essentially required to train the system in such a way that it can segment the image with high accuracy, even in the presence of noise.

The proposed approach uses EM algorithm to process the initial labels selected by user. MGH-based image features have been extracted, and most relevant and useful image descriptors are selected by employing GA. Selected image descriptors and targets have been given as input to a neural network for generation of FIS. The generated FIS hence used for segmentation. IMT values have been measured from the proposed RSC-US approach segmented images. Based on measured IMT values, these images have been classified into abnormal or normal subjects by SVM classifier. Segmentation and classification results are compared with some state-of-the-art segmentation techniques. The obtained segmentation and classification results indicate the usefulness of the proposed approach. The flowchart of the proposed RSC-US approach is depicted in Fig. 1. The individual phases of the proposed approach are explained in the following subsections.

2.1 Label initialization of pixels

In first phase of the proposed technique, initially user has selected the various regions from carotid artery ultrasound image, and a specific label has been assigned to every selected part of image. Due to overlapping of organs, the assigned labels might be inaccurate. Therefore, the labels

Fig. 1 Block diagram of the proposed RSC-US approach

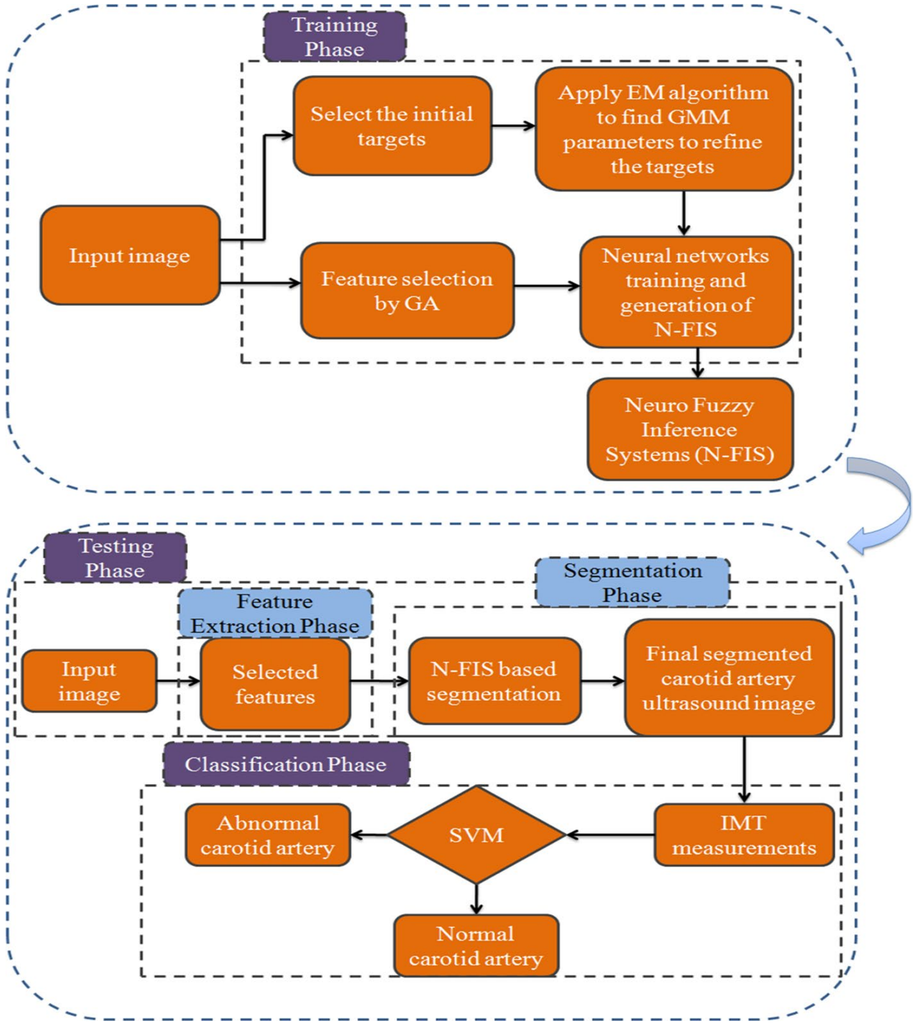

assigned by the users have been further processed to find more accurate labels. Figure 2 shows the sample carotid artery ultrasound image in which different parts of image has been selected, and every part has assigned a specific label. The carotid artery ultrasound images mainly have three classes: the arterial wall, area inside artery, and background tissues. Figure 2 shows the initial selected labels having some overlapping regions. In particular, some pixels of other classes are merged into the artery wall which have high impact because narrowing of the artery causes owing to the thickness of arterial walls.

The probability of merging pixels of other classes into arterial walls is higher, owing to the narrow region of arterial walls and background tissues. The other regions like background tissues and inside arterial walls have large areas, and merging probability is low for these classes. The probability of merging pixels between regions should be minimized by refining the initially selected labels. For this purpose, EM algorithm has been used to handle this issue.

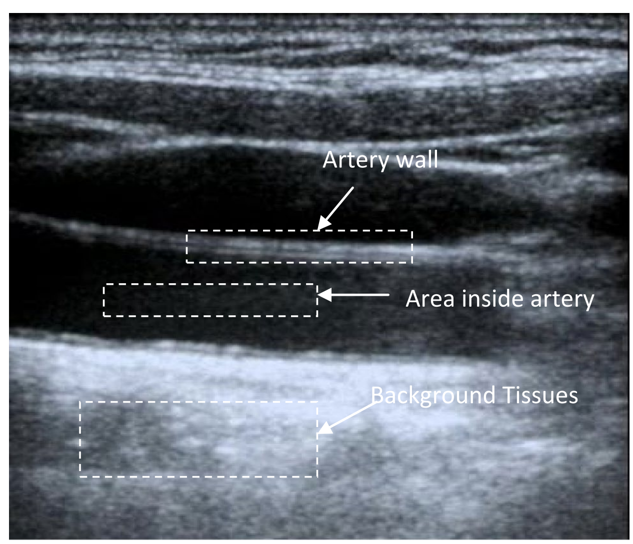

Fig. 2 Initial targets marked as artery wall, area inside the artery and the background tissues

2.2 The expectation maximization step

The EM algorithm is widely used to estimate the statistical models. It has the advantage of being robust, simple and easy to implement. EM algorithm has capability to perform well at ultrasound images. The objective of using EM algorithm is to find iterative convergence of a set of input projections on the most likely reconstruction. The goal is to estimate the parameters of Gaussian mixture model (GMM) by applying EM algorithm which will further be used for target class estimation. The unknown parameter θ of the model needs to be estimated in a way that $p(\mathbf{X}|\theta)$ becomes maximized. Log-likelihood function is utilized to estimate the parameter θ as described in Eq. (1).

$$L(\theta) = \ln \cdot p(\mathbf{X}|\theta) \tag{1}$$

At given data $\mathbf{X}$, the parameter θ can be considered as a function of log likelihood. The logarithmic function is strictly increasing and so that value of θ maximizes $p(\mathbf{X}|\theta)$. Hence, $L(\theta)$ will become maximum. EM algorithm iteratively maximizes $L(\theta)$. Further, it is assumed that after last iteration, the current estimate of θ becomes θ_n.

$$L(\theta) > L(\theta_n) \tag{2}$$

Mathematically, the difference should have to be maximized using Eq. (3),

$$L(\theta) - L(\theta_n) = \ln \cdot p(\mathbf{X}|\theta) - \ln \cdot p(\mathbf{X}|\theta_n) \tag{3}$$

The sole objective is to select the values of θ parameter, at which $L(\theta)$ get maximized. EM algorithm is used to select θ at maximum $L(\theta|\theta_n)$. The updated value is represented by θ_n and finally got,

$$\begin{aligned}\theta_{n+1} &= \arg\max_{\theta} \{l(\theta|\theta_n)\} \\ &= \arg\max_{\theta} \left\{ L(\theta_n) + \sum_{z} p(z|\mathbf{X}, \theta_n) \ln p(\mathbf{X}|z, \theta) \right. \\ &\qquad \left. p(z|\theta) \big/ p(\mathbf{X}|\theta_n) p(z|\mathbf{X}, \theta_n) \right\}\end{aligned}$$

The constant terms w.r.t. θ need to be dropped.

$$\begin{aligned}&= \arg\max_{\theta} \left\{ \sum_{z} p(z|\mathbf{X}, \theta_n) \ln p(\mathbf{X}|z, \theta) p(z|\theta) \right\} \\ &= \arg\max_{\theta} \left\{ \sum_{z} p(z|\mathbf{X}, \theta_n) \ln p(\mathbf{X}, z, \theta) \big/ p(z, \theta) p(z, \theta)/p(\theta) \right\} \\ &= \arg\max_{\theta} \left\{ \sum_{z} p(z|\mathbf{X}, \theta_n) \ln p(\mathbf{X}, z|\theta) \right\} \\ &= \arg\max_{\theta} \left\{ E_{Z|X,\theta_n} \ln p(\mathbf{X}, z|\theta) \right\}\end{aligned} \tag{4}$$

The E and M steps are apparent in Eq. (4). The term $E_{Z|\mathbf{X},\theta_n}$ is the conditional probability of finding the labels Z on certain iteration (θ). The EM algorithm comprises of the following steps:

1. Expectation step, which is used to find the conditional expectation $\{E_{Z|\mathbf{X},\theta_n} \ln p(\mathbf{X}, z|\theta)\}$.
2. Maximization step, which maximizes the step 1, w.r.t. θ.

Further details and derivation of EM algorithm can be found in [5, 28]. Using EM algorithm, mean and standard deviation for GMM model have been estimated. These estimated parameters are then used in the following expressions to find more refined labels for the input data.

$$z_{ik} = \sqrt{\sum_{j=1}^{n} \left[\mathbf{X}_{ij} - u_k/\sigma_k\right]^2} \quad \text{for } k = 1, 2, \ldots, l \tag{5}$$

where $\mathbf{X}_{ij}$ is the jth element of the ith input data point and k is the number of class, u and σ are the mean and standard deviation, respectively, estimated previously (preceding iteration) by the EM algorithm. The predicted labels are calculated by using the following expression:

$$y_k(\mathbf{X}_i) = 1/1 + (z_{ik}/f_{\mathrm{d}})^{f_{\mathrm{e}}} \tag{6}$$

where y_k represents the membership of each pixel to a certain class k, and z_{ik} values are obtained from Eq. (5). The variables f_{e} and f_{d} are used for controlling the fuzziness amount and these values are set empirically [32]. It is obvious that the output of y_k will be in the interval of 0 and 1. Using the maximum value of index y_k, we get the target label associated with each pixel. The graphical representation GMM estimated by EM algorithm is presented in Fig. 3, where horizontal axis ($\mathbf{X}$) shows the number of data points in association with its probability density function at vertical axis, and the dotted curves represent each cluster.

2.3 Feature extraction

The objective of this phase is to formulate a feature vector for every pixel, hence used for segmentation. In this study, feature extraction strategy based on MGH has been used. These extracted features have advantage to represent the medical images [18, 22].

2.3.1 *Moments of gray-level histogram image descriptors*

Statistical image descriptors are being used in image analysis. These features are based on the intensity histogram and are extracted for every pixel. The histogram-based features have better capability to represents the normal and abnormal tissues in medical image. Nine MGH features are

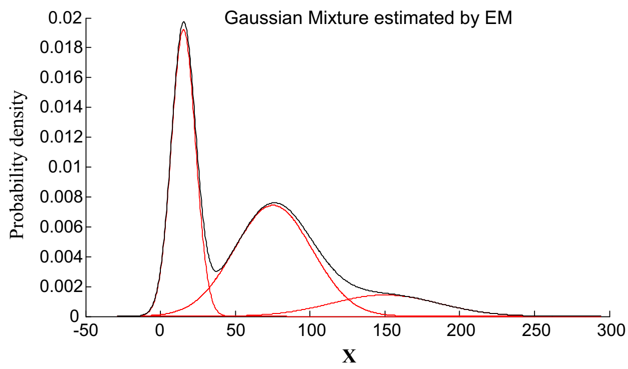

Fig. 3 Graphical representation of parameters estimation using EM algorithm

extracted from the given image [18]. The nth-order statistical moment about mean can be computed by using the following equation:

$$u_n = \sum_{i=0}^{L-1} (z_i - m)^n \cdot p(z_i) \tag{7}$$

where $p(z_i)$ is the histogram of image intensity level in a certain region, and z shows the intensity. L represents the possible intensity levels and m is an average intensity value.

A total of nine MGH features are extracted from the input image. Mathematical description of each feature is as under:

$$\text{Mean} = \text{FM1} = \sum_{i=0}^{L-1} z_i \cdot p(z_i) \tag{8}$$

$$\text{Standard Deviation (SD)} = \text{FM2} = \sqrt{u_2} \tag{9}$$

$$\text{Smoothness} = \text{FM3} = 1 - 1/1 + \sigma \tag{10}$$

$$\text{Third moment} = \text{FM4} = \sum_{i=0}^{L-1} (z_i - m)^3 \cdot p(z_i) \tag{11}$$

$$\text{Uniformity} = \text{FM5} = \sum_{i=0}^{L-1} p^2(z_i) \tag{12}$$

$$\text{Entropy} = \text{FM6} = -\sum_{i=0}^{L-1} p(z_i) \cdot \log_2(p(z_i)) \tag{13}$$

$$\text{FM7} = \sum_{i=0}^{L-1} p^3(z_i) \tag{14}$$

$$\text{FM8} = \sum_{i=0}^{L-1} p^4(z_i) \tag{15}$$

$$\text{FM9} = \sum_{i=0}^{L-1} p^5(z_i) \tag{16}$$

where FM represents feature moment of MGH. A (5×5) window size is used for feature extraction and important features are selected using GA and thus used for segmentation of carotid artery ultrasound images. The mentioned window size offers better segmentation results on ultrasound images [15, 18].

2.4 Feature selection

Feature selection has been carried out to reduce the feature vector dimensionality while preserving the accuracy. In order to improve computational cost and save valuable resources, irrelevant and redundant features might be omitted by utilizing searching algorithms. Many feature selection strategies have been explored by various researchers in the literature including sequential backward selection, greedy stepwise, forward selection, genetic algorithms, and swarm optimization, whereby each technique has its own advantages and disadvantages [27].

In this study, GA has been used to select discriminating image descriptors from the already extracted feature set and hence used for segmentation. WEKA, a machine learning software, has been employed for this purpose [17]. GA parameters are set empirically and the following configuration parameters of GA have been used for feature selection. Except the following (probability of crossover = 0.8, number of generations = 100, Population size = 100 and probability of mutation = 0.1), default GA parameters of WEKA have been used.

Only 4 out of 9 features have been selected by GA and used for segmentation, which obviously saves time and resources. The following features, namely FM2, FM4, FM5, and FM6, have been selected by GA and thus used for segmentation.

2.5 Neuro-fuzzy classifier

In this research, NFC has been used for classification of the input feature vector. In image segmentation, the effectiveness of the NFC approach has been analyzed. The basic objective of fuzzy classification is to segment out the feature space into specified fuzzy classes. Due to the overlapping nature of medical images, it is possible that a pixel may belong to various clusters with different degree of membership. In this scenario, fuzzy approaches might be suitable approaches [34, 43]. Like other fuzzy techniques, in NFC, fuzzy *if* then *else* rules are applied to develop a classifier. NFC-based segmentation needs a FIS which is actually a collection of fuzzy rules.

NFC is a supervised learning approach. It has a similar structure (i.e., input, hidden, and output layers) like other neural networks. Inputs to the classifier are optimized features selected by GA and a hidden layer of 50 neurons. Output layer consists of three neurons, which represents three different classes of carotid artery ultrasound image. Neural networks have the capability of efficiently learning the behavior of a system and it can successfully generate the fuzzy "*if* then *else* rules" and fuzzy membership functions. The general structure of NFC is as below:

Input layer: Four neurons;
Hidden layer: Fifty neurons;
Output layer: Three neurons.

In order to find optimal number of hidden layer neurons, validation set error has been used. In this process, various input and hidden layers neurons combinations are compared. This process has been repeated for a number of times with leave-one-out strategy, and the model with minimum mean sum of prediction error (MSPE) is selected [3, 39]. During the training process of NFC, the given dataset associated its labels which are obtained by the EM model. To obtain the optimal neural network structure, we have computed the mean square prediction error (MSPE) from the given dataset by varying the number of hidden layer neurons. The prediction errors like MSPE can be obtained by using cross-validation technique of leave out one approach. The average MSPE on the M subsets that have been left out defines the cross-validation error, CV:

$$\mathrm{CV} = \frac{1}{M}\sum_{m=1}^{M} \mathrm{MSPE}_m$$

The model with minimum cross-validation error has been selected; hence, enhanced classification accuracy has been achieved utilizing the above-mentioned architecture obtained by the aforementioned procedure.

2.5.1 NFC training and testing

After the selection of important image descriptors using GA, NFC training and validation procedure start. Class labels have been assigned to every pixel by EM algorithm. For training and validation of NFC, 18 different carotid artery images have been utilized from obtained dataset. Training and validation process was performed at the ratio of 67 and 33 %, respectively. The FIS was generated by NFC and further used for segmentation of carotid artery ultrasound images. Root-mean-square error (RMSE) has used measure the difference between actual and predicted

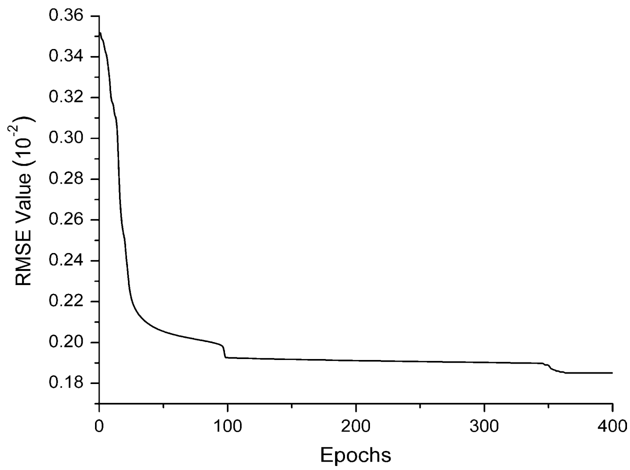

Fig. 4 RMSE curve of NFC training at different epochs

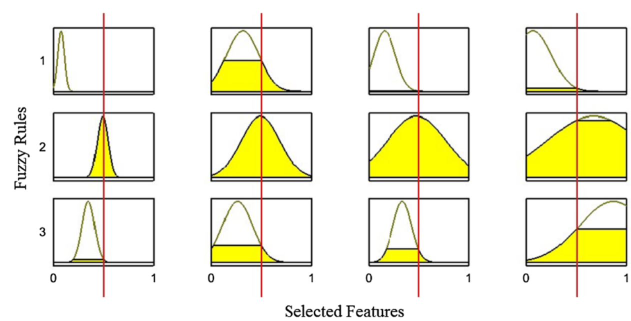

Fig. 5 NFC generated fuzzy inference system (FIS) for segmentation

values. Figure 4 shows RMSE curve plotted against epochs of NFC training. From Fig. 4, it can be observed that NFC converges when error gradient becomes very small. RMSE shows monotonically decreasing behavior; therefore, error rate decreases with increasing number of epochs. NFC was trained at 400 epochs, so it can learn the patterns effectively.

FIS has been generated and utilized to segment the carotid artery ultrasound images. The proposed RSC-US approach is tested on significant amount of data which is described in Sect. 2.3.1. The proposed technique's generated FIS is shown in Fig. 5. The horizontal axis shows the number of selected image descriptors by GA, whereas the vertical axis shows the number of fuzzy rules used for classification of the input data. The input feature values were scaled into the range of 0 and 1, and Fig. 5 shows the visual representation of fuzzy rules. The index line indicates which rule might be activated for input data, and it may change for every input instance. The shaded region of the membership function shows visually apparent fuzzy membership value. The fuzzy rule view is used to interpret the overall fuzzy inference process at once. There are

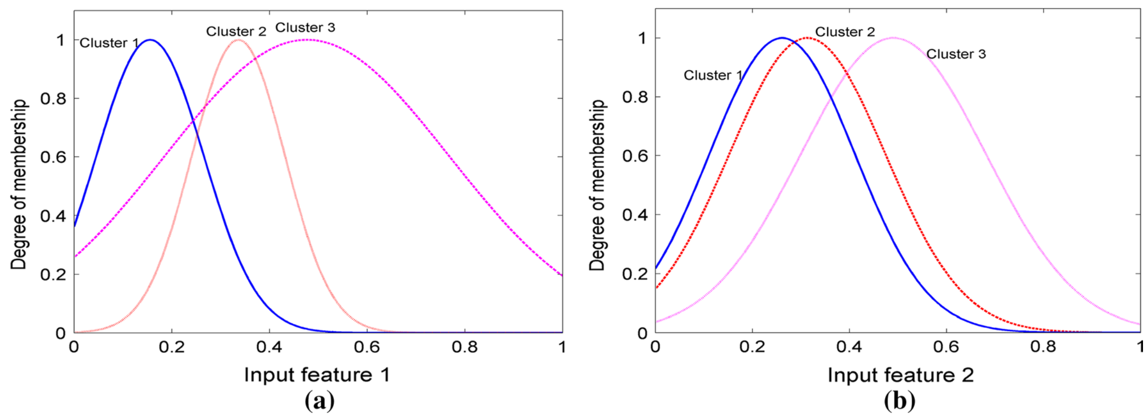

Fig. 6 Graphical representation of fuzzy membership functions for selected feature 1 and 2 respectively

three fuzzy rules incorporated in FIS which are further used for classification (segmentation) of input data. The graphical representation of fuzzy membership functions for the selected feature 1 and feature 2 are shown in Fig. 6 respectively. Similarly, fuzzy membership functions for feature 3 and 4 are designed for the classification of input features.

2.6 Classification of segmented carotid artery ultrasound images

The proposed approach segmented images needs to be classified into abnormal or normal subjects. For this purpose, IMT values need to be measured from segmented images. Feature vector based on IMT values is formed and fed as an input to SVM classifier. Therefore, SVM has advantages over other classifiers because of its enhanced learning capability. Hence, SVM is used for classification of segmented images.

Five different commonly used features namely mean, variance, standard deviation, max, and min are extracted from measured IMT values and fed as input to the classifier. The extracted feature values are normalized into the range of [0–1]. By utilizing these features, SVM offers superior classification accuracy.

2.6.1 Support vector machine (SVM) classifier

SVM classifier is a supervised learning algorithm, which is successfully being used for classification and analysis of data. Originally, SVM is a binary classifier, but with kernel method, it can be utilized for multi-class problem as well. For instance, to classify data into two classes, SVM finds a new hyper-plane with the help of support vectors and margins. SVM selects the hyper-plane with maximum separation between the classes. During classifier training, classification error is minimized at each new training instance to find the optimal linear hyper-plane [2, 12, 31].

Different kernel functions are available for SVM classifier to classify the data. In current research, we have used SVM-radial basis function kernel (SVM-RBF) for classification of segmented carotid artery ultrasound images. Further, LIBSVM 3.11 toolbox was used for training and testing of SVM classifier [9, 16]. In this study, tenfold cross-validation has been used to train SVM classifier.

2.7 Classification performance measures

In statistical prediction, various cross-validation techniques are reported in the literature to assess the usefulness of the classification model. Among these, jackknife test is a popular one as it offers a stringent test. It is widely used by analysts to authenticate the prediction accuracy. In this work, jackknife cross-validation technique has been used to examine the classifier excellence. Jackknife test utilizes $N-1$ samples for model training, while the Nth sample is used for testing. The class of test sample is predicted by the classifier based on $N-1$ training samples, and the process is repeated for N times. The true positive (TP) and true negative (TN) represent correct classification for both positive and negative classes, respectively, whereas false positive (FP) and false negative (FN) represent the samples, which are incorrectly classified by the model. Following measures have been computed for classification assessment.

Accuracy It is used to assess the effectiveness of the classifier, and it can be computed by the following expression:

$$\text{Accuracy} = (\text{TP} + \text{TN})/(\text{TP} + \text{FP} + \text{TN} + \text{FN}) \times 100 \tag{17}$$

Sensitivity Sensitivity checks the ability of a classification model to identify the positive class patterns, and it can be calculated by the given equation.

$$\text{Sensitivity} = \text{TP}/(\text{TP} + \text{FN}) \tag{18}$$

Specificity It checks the capacity of a classifier to identify negative patterns of the given dataset, and it can be computed by the following formula:

$$\text{Specificity} = \text{TN}/(\text{TN} + \text{FP}) \tag{19}$$

Matthews correlation coefficient (MCC) It is used for assessment of binary classification and has a range of '−1' to '1,' where '1' value refers to accurate pattern prediction, '0' indicates a random classification accuracy, and '−1' refers to misclassification. MCC value can be computed by the following equation:

$$\text{MCC} = (\text{TP} \times \text{TN}) - (\text{FP} \times \text{FN}) \Big/ \sqrt{(\text{TP} + \text{FN})(\text{TP} + \text{TP})(\text{TN} + \text{FN})(\text{TN} + \text{FP})} \tag{20}$$

The F-measure It considers recall and precision to assess the prediction of a classifier by taking the average of both and has a range of [0–1]. Worst and best scores are represented by '0' and '1,' respectively. It can be calculated using the given equation:

$$\text{precision} = \text{TP}/(\text{TP} + \text{FP}) \tag{21}$$

$$\text{recall} = \text{TP}/(\text{TP} + \text{FN}) \tag{22}$$

$$F\text{-score} = 2 \times \text{precision} \times \text{recall}/\text{precision} + \text{recall} \tag{23}$$

ROC and area under the curve (AUC) ROC is the graphical representations of false and true positive rates and provides effective indicators in clinical testing. ROC and its associated indices are widely used for evaluation of the radiological tests, which helps in demonstrating how accurately a classifier performs the classification task.

Several indices can be associated with ROC, whereby one of the popular index measures is area under the curve (AUC) [35]. It is used to measure the overall performance of diagnostic test. To check the effectiveness of the classifier, AUC has also been calculated from ROC curve.

3 Results

Real carotid artery ultrasound images have been segmented by the proposed RSC-US approach. Detail of the dataset used in this experiment is as under:

3.1 Datasets

The carotid artery ultrasound imaging dataset was obtained from Shifa International Hospital, Islamabad, Pakistan. Imaging equipment of Toshiba's Xario XG with linear probe transducer with a frequency range of 7–8 MHz has been used in the said hospital for carotid artery ultrasound imaging. The videos have been recorded for 10 s and then converted into frames by employing video decompiler. In this experiment a total of 57 subjects' data has been utilized. The dataset contains a total of 300 images in which 140 are normal and 160 are abnormal. With the help of medical experts of the said hospital only few 3–6 frames (images) of each subjects' has been identified and hence used for experiment. The extracted frames are labeled by the expert as normal or abnormal frames (images) which are then used for model evaluation. The obtained images have size of 800 × 600 with pixel resolution of 72 pixels per inch (PPI). The original images have been cropped and resized to 350 × 380. Subjects' involved in the experiment has the age range of 35–74 years with mean age of 55.75 years and standard deviation of 9.43 years. To check the performance of the proposed RSC-US scheme classification results are compared against already labeled images. All computations were performed on an Intel Core i7 Pc with MATLAB 7.12 (2011a).

3.2 Real carotid artery images segmentation

The dataset described in Sect. 3.1 has been segmented by the proposed RSC-US technique. To confirm robustness of the proposed approach, it has been evaluated by considering various intensities of Gaussian noise. The results of the proposed technique have been compared with state-of-the-art techniques. The proposed RSC-US technique outperforms both at noisy and noise free images.

Figure 7a shows one of the original longitudinal carotid artery ultrasound images with marked plaque in carotid artery. Selected ROI is shown in Fig. 7b. Segmented carotid artery ultrasound image by the proposed technique is presented in Fig. 7c. The proposed technique successfully separated plaque in carotid artery with minimum misclassifications compared to other techniques. The proposed approach obtained segmentation results are compared with some exiting state-of-the-art techniques. Figure 7d–f shows the image segmented by the FCM, *K*-means and sFCMLSM methods, respectively. From visual inspection, superiority of the proposed RSC-US approach is clear. On the other side, FCM, *K*-means, and sFCMLSM segmented images contain much misclassified patterns especially in marked plaque area. Further, IMT has been measured from the

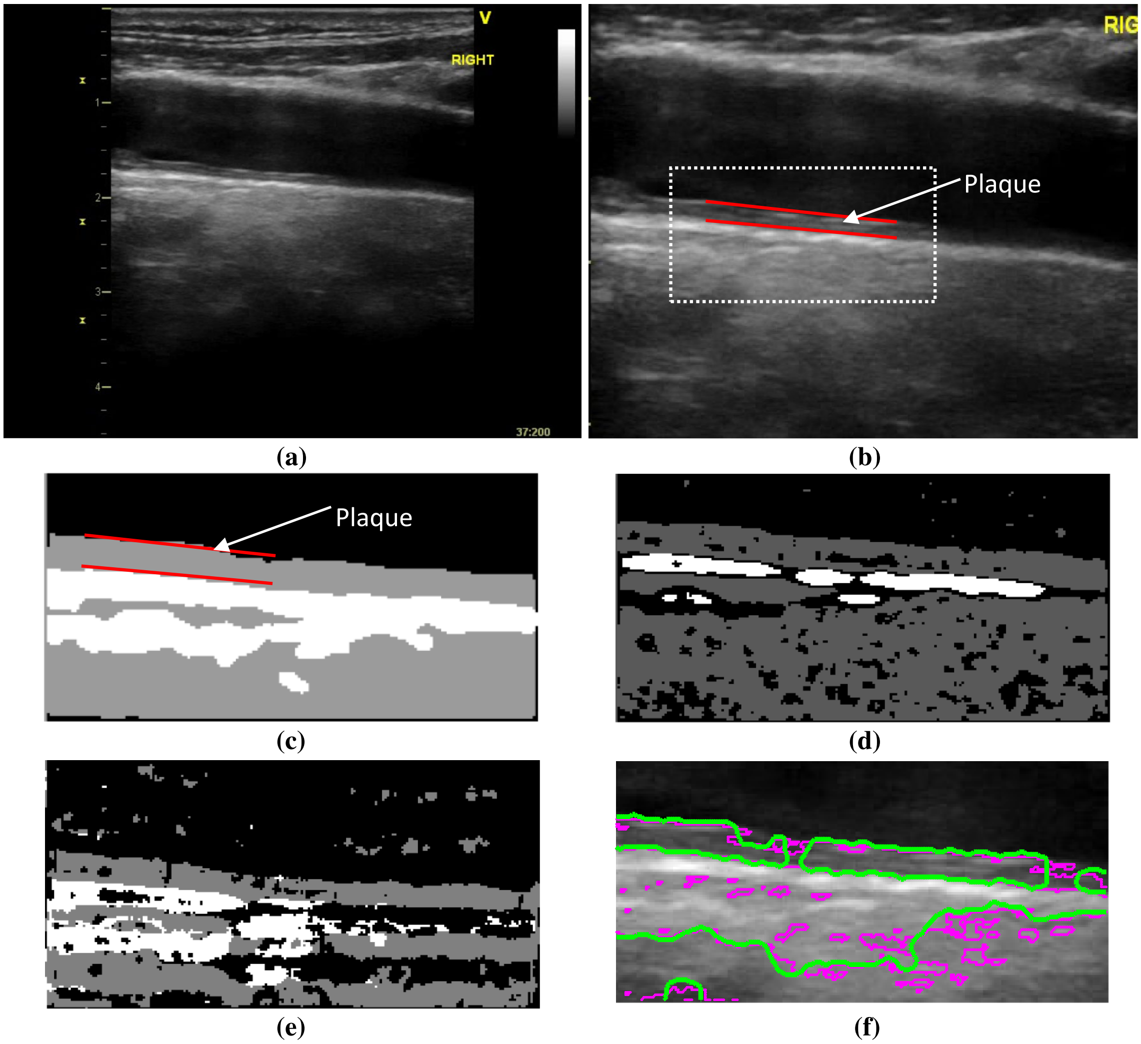

Fig. 7 **a** One of the longitudinal original carotid artery ultrasound images with marked plaque, **b** selected ROI, **c** segmented by the proposed RSC-US scheme, **d** FCM segmentation, **e** *K*-means and **f** *magenta* represents initial and *green* represents final segmentation of sFCMLSM technique (color figure online)

segmented images to form a feature vector and fed as input to SVM classifier. Since, image post-processing techniques are highly dependent on segmentation quality. If carotid artery segmented images contains misclassifications, IMT value may not be accurately measured. Consequently, the effect of the inaccurate IMT measure will result in the form of misleading results. Particularly, dealing with medical images a great care is needed because wrong predictions may not be affordable in this field.

Medical images contain various types of limitations, for instance, ultrasound images are of lower quality, are degraded with noise, and have wave interferences. To check the robustness of the proposed technique, images have been corrupted with white Gaussian noise of various intensities. Keeping in mind, medical images may not contain high intensity of noise, beside this; we have checked the proposed technique at Gaussian noise of variance 0.01, 0.015, 0.05 and 0.1. Noisy variants of carotid artery images segmented by the proposed RSC-US approach with Gaussian noise of variance 0.05 are shown in Fig. 8. It can be observed from Fig. 8 that the proposed technique has successfully segmented noisy versions of carotid artery ultrasound images.

Figure 9a shows one of the original longitudinal carotid artery ultrasound images. The image has been corrupted with Gaussian white noise of variance 0.10 and selected ROI is shown in Fig. 9b. Images segmented using the proposed RSC-US, FCM, *K*-means, and sFCMLSM approaches are shown in Fig. 9c–f respectively. Apparently, it can be observed that the image segmented by the proposed approach outperform all the mentioned techniques with minimum misclassifications even in the presence of

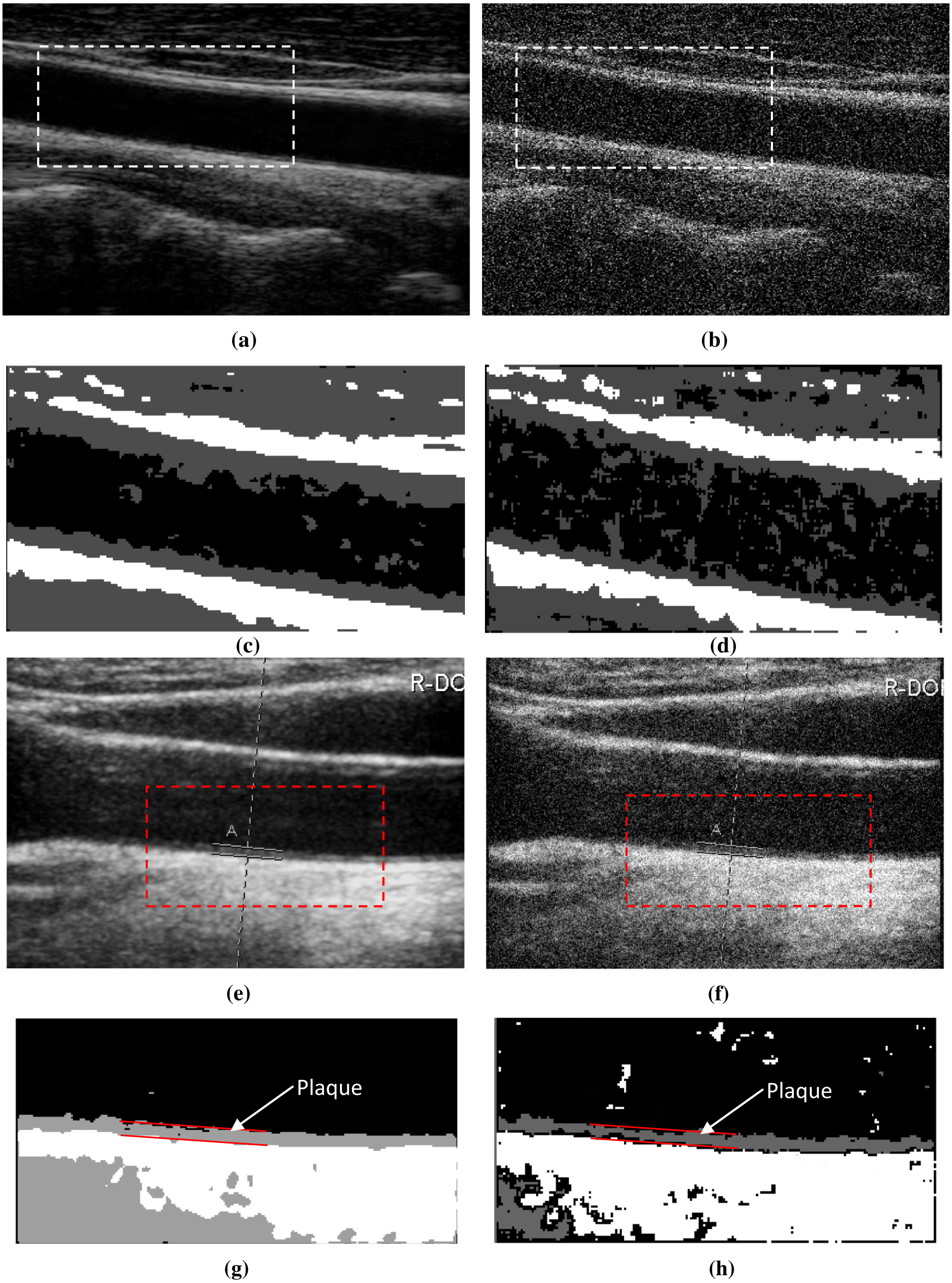

Fig. 8 Sample noise free and noisy longitudinal carotid artery images segmented by the proposed RSC-US approach. **a** Original carotid artery image with selected ROI, **b** noisy carotid artery image with Gaussian noise of 0.05 variance, **c** segmentation of **a** by the proposed approach, **d** the proposed approach segmentation of **b**, **e** original carotid artery image with selected ROI, **f** Noisy carotid artery image with Gaussian noise of 0.05 variance, **g** the proposed approach segmentation of **e** image, **h** segmentation of noisy image **f** by the proposed approach

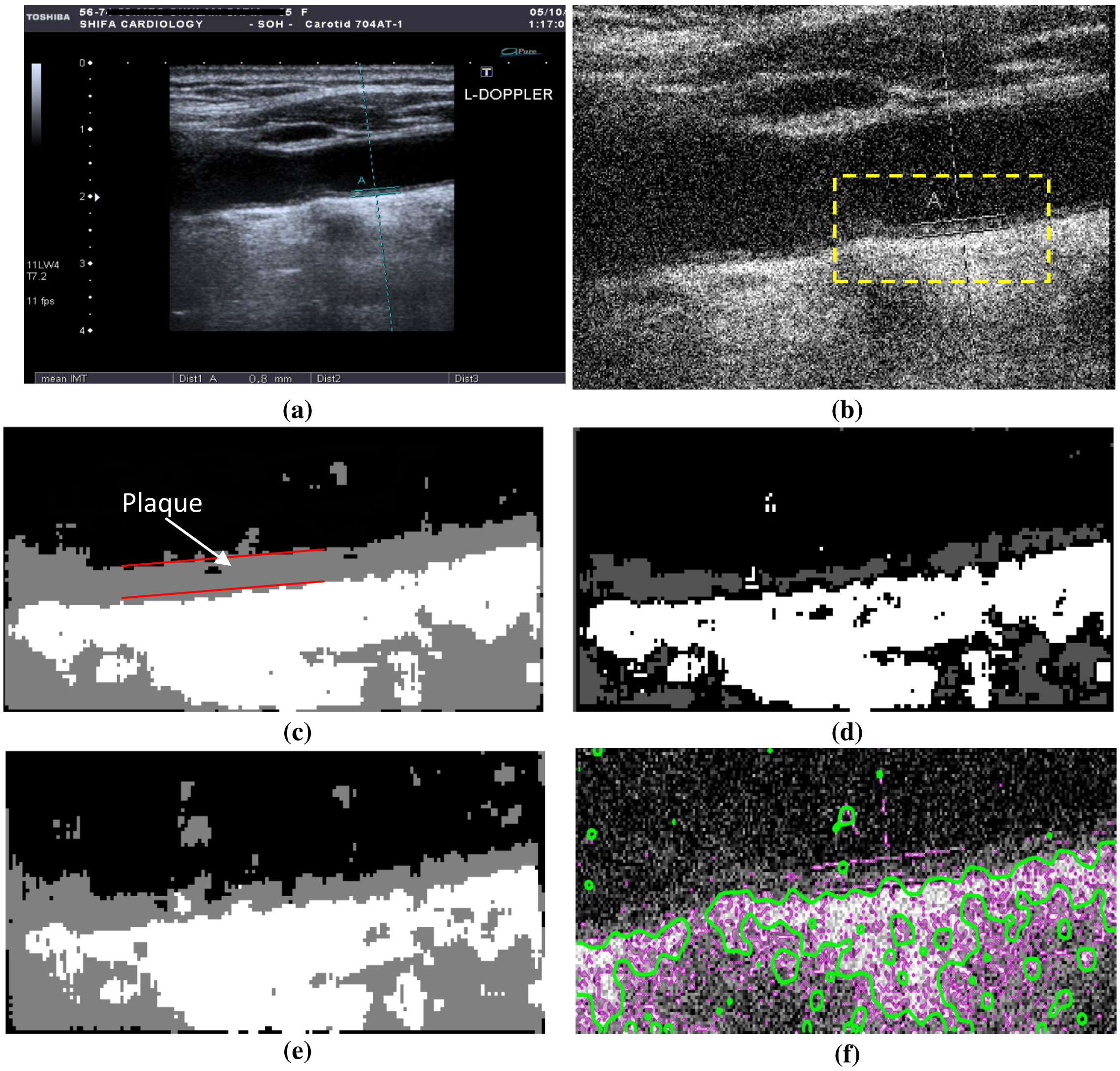

Fig. 9 **a** One of the original longitudinal carotid artery ultrasound images, **b** image corrupted by Gaussian noise of variance 0.10 and selected ROI, **c** the proposed RSC-US technique segmented image, **d** FCM segmentation, **e** *K*-means and **f** sFCMLSM segmentation

noise. In Fig. 9d, FCM segmented image has a lot of misclassified regions; hence, IMT may not measure accurately. Other segmentation approaches, such as *K*-means, Fig. 9e and sFCMLSM Fig. 9f, we can also observe the existence of misclassified pixels. These noisy patterns may mislead IMT measurements and consequently, may increase the false detection of plaque in carotid artery. Segmentation performance, in the presence of noise, shows the robustness and effectiveness of the RSC-US approach.

3.2.1 Performance analysis using segmentation quality measure

By visual inspection, we have observed that the proposed RSC-US technique outperform the other techniques at different noise levels. To verify the superiority of the proposed approach qualitatively, DBI of segmented images has been determined. DBI is the ratio of sum of within and between clusters. Smaller the values of DBI better the clustering quality [13]. Table 2 shows DBI average performance of different techniques for the obtained dataset of 300 real carotid artery ultrasound images on various noise levels. From Table 2, it can be observed that the proposed RSC-US outperforms all mentioned technique at all given noise levels. From the results presented in Table 2, a significant fact is established that the noise has minimum effect on the proposed approach compared to the other considered techniques. Hence, RSC-US segmentation shows the superiority in terms of quantitative quality measures. The graphical representation of segmentation quality measure

Table 2 Average performance comparison of the proposed RSC-US and other techniques over 300 carotid artery ultrasound images

Gaussian noise levels	Segmentation techniques				
	Davies–Bouldin index (DBI)				
	FCM	sFCM	*K*-means	sFCMLSM	The Propsoed RSC-US
Original image	0.4653	0.5660	0.4640	0.4710	0.4379
0.01	0.4772	0.5921	0.4739	0.4835	0.4417
0.02	0.4922	0.6341	0.4911	0.5002	0.4527
0.05	0.5213	0.7971	0.5171	0.5514	0.4783
0.10	0.5926	0.9582	0.6041	0.6127	0.4826

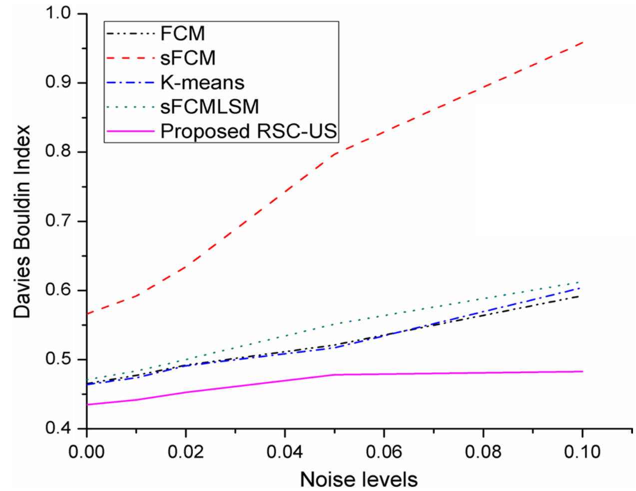

Fig. 10 Segmentation quality comparison of different techniques at various noise levels

based on DBI at various noise levels is shown in Fig. 10. It is evident from Fig. 10 that the proposed segmentation approach works efficiently in the presence of noise.

Segmentation time (in s) of the proposed RSC-US technique across the increasing number of features is shown in Fig. 10. Only four out of nine optimal features have been selected by GA and offered better segmentation results. It is obvious that fewer features require less segmentation time and save valuable resources; however, it may affect the segmentation accuracy. It is evident from Tables 2, 3, and 4 that the proposed approach at reduced features maintains accuracy; hence offer superior segmentation and classification results. Thus, as shown in Fig. 11, the proposed RSC-US outperforms the other segmentation techniques in term of computational time which shows its effectiveness.

3.3 Effects of segmentation on classification

Accurate segmentation would surely be effective for post-processing techniques. To investigate this, we have evaluated classification performance using different segmentation algorithms.

To classify the segmented carotid artery image as normal or abnormal, IMT has been measured from segmented carotid artery images. ROI (arterial walls) should be successfully separated from background tissues with minimum misclassifications. For instance, in current scenario; object of interest in carotid artery images is plaque in the carotid artery. Successful segregation of ROI contributes a lot to IMT measurements with higher level of confidence. Consequently, its affect will be in the form of better classification. The mean and standard deviation of measured IMT values for normal carotid artery dataset are 0.392 and 0.109 mm, respectively. Whereas, for abnormal carotid artery, the mean and standard deviation of measured IMT values are 0.745 and 0.173 mm, respectively. Figure 12a, b shows the graphical representation of the IMT measurements for one of the normal and abnormal carotid artery ultrasound images.

Table 3 Effect of segmentation on object classification

Segmentation techniques	Classification techniques		
	Accuracy (%)		
	SVM	KNN	MLBPNN
FCM	96.40	95.50	95.91
K-means	95.20	94.37	94.63
sFCMLSM	96.80	95.78	96.00
Proposed RSC-US	98.84	98.30	98.40

Table 3 shows the performance comparison of SVM, KNN, and MLBPNN classifiers based on various segmentation approaches. It is clear from Table 3 that every classifier offers higher accuracy based on the proposed approach segmentation. It is due to the fact of better segmentation quality produced by the proposed RSC-US approach in contrast to FCM, *K*-means, and sFCMLSM techniques. Effect of the segmentation on classification is shown in Fig. 13. It can be observed from Fig. 13 that the proposed segmentation approach-based classification offers superior performance for all classifiers.

In this paper, various classifiers are employed including SVM to separate the abnormal subjects from normal ones. To choose an optimum classifier for carotid artery ultrasound images, performance of each classifier in terms of various quality measures has been analyzed on the proposed segmentation approach. Table 4 shows the performance comparison of SVM, MLBPNN, and *K*-nearest neighbor (KNN) approach at various classification quality parameters. The classification accuracy generated by SVM on the dataset is 98.84 %.

Table 4 Classification performance comparison of SVM, KNN, and MLBPNN using the proposed RSC-US segmentation technique

Techniques	Accuracy (%)	*F*-score	MCC	Sensitivity	Specificity
KNN	98.30	0.9700	0.9483	0.9697	0.9486
MLBPNN	98.40	0.9551	0.9127	0.9750	0.9385
SVM	98.84	0.9880	0.9767	1.0000	0.9773

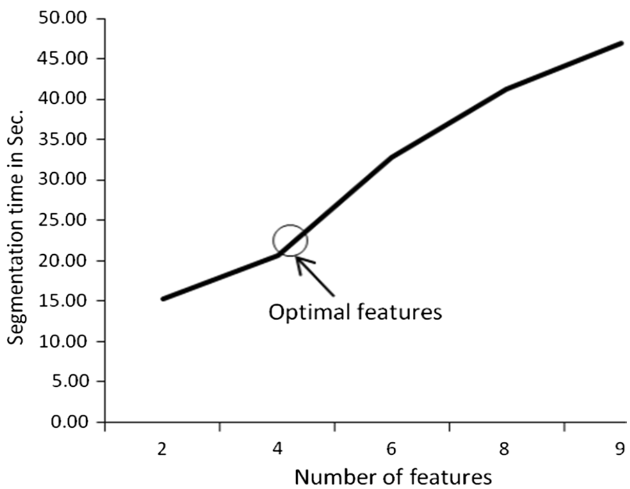

Fig. 11 Computational time (in s) of the proposed scheme across different number of extracted features

Further, a comparison of different classifiers in term of ROC and AUC has also been made. Figure 14 shows ROC curves for SVM, MLBPNN, and KNN classifiers. From Fig. 14, it can be seen that SVM's ROC is close to vertical axis, which depicts high classification accuracy. Obtained AUC value of 0.98 shows the overall better diagnostic test and confirmed the advantage of the proposed scheme.

The effect of segmentation at classification has been analyzed, and it can be observed that the proposed segmentation technique-based classification offers superior performance. As described earlier, the post-processing techniques are highly dependent upon quality of segmentation. In this research work, images have been segmented by different techniques namely: FCM, *K*-means, sFCMLSM, and the proposed RSC-US algorithms. Statical analysis of classification results reveals that the proposed segmentation technique-based classification performance improved by a margin of 2.47–4.00 % (Fig. 13; Table 3). This significant improvement in classification is largely due to the correct segmentation of carotid artery ultrasound images.

4 Discussions

In this research work, we have proposed a new hybrid method for carotid artery ultrasound image segmentation. The proposed method utilizes the EM to find accurate class labels for each pixels, and GA has been used to select the important image features. FIS has been generated by NFC to segment the carotid artery ultrasound images. From segmented images, IMT values are measures and feed as input to the SVM classifier for normal and abnormal subject segregation.

The proposed method is tested against 300 real carotid artery ultrasound images, and from obtained results, we have observed that the proposed method outperform the other techniques in term of visually and quantitatively. From Fig. 7c, it can be observed that the proposed approach accurately segmented the plaque in carotid artery. It is due

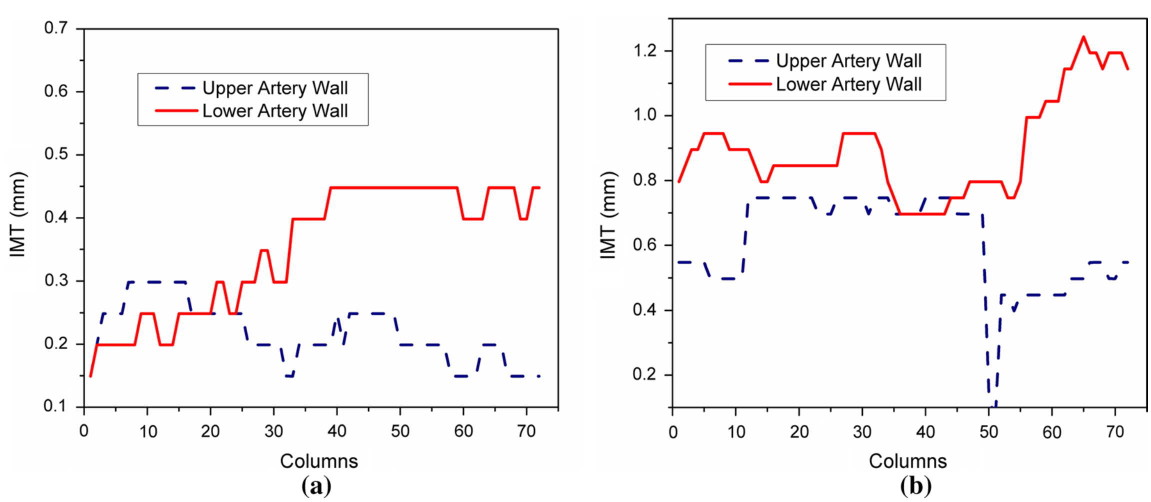

Fig. 12 **a** IMT values of the plaque of a normal and **b** abnormal carotid artery

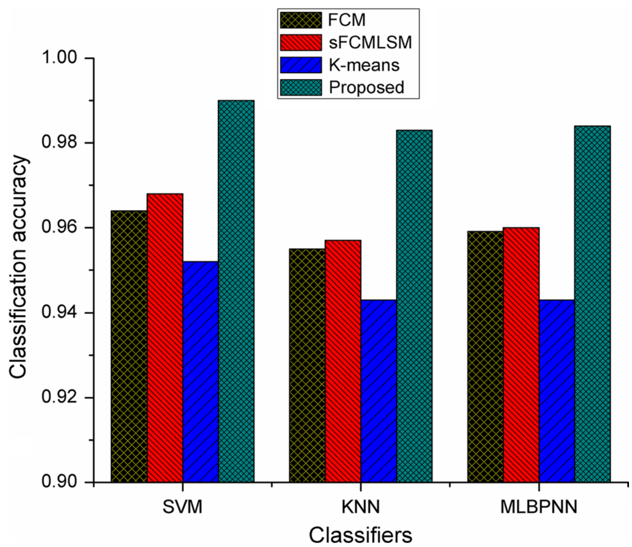

Fig. 13 Comparison of classification accuracy using different segmentation techniques

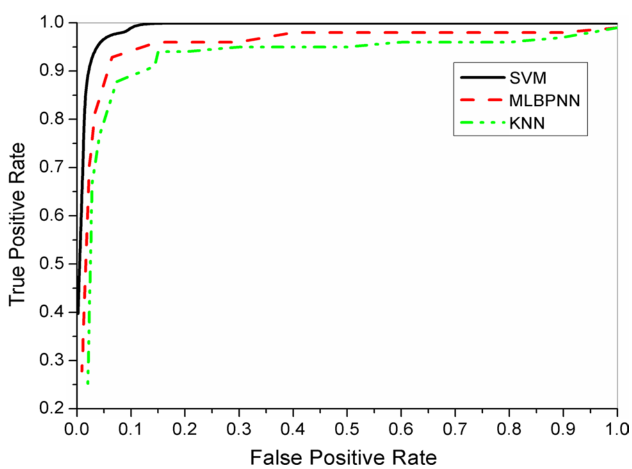

Fig. 14 ROC curves of SVM, MLBPNN, and KNN

to the fact that the well-trained model of NFC which utilizes the most important image descriptions. The plaque in carotid artery is separated successfully an accurate IMT values can be obtained from segmented image, hence used for classification.

Ultrasound images contain various types of inherent degradations like, presence of noise and low quality. The proposed approach shows robustness and successfully segmented the carotid artery ultrasound images in the presence of various intensities of Gaussian noise. It is evident from Figs. 8c–e, h and 9c that the proposed technique outperform the other technique.

To validate the effeteness of the proposed approach quantitatively, we have used DBI as a clustering quality measure. Table 2 shows the average DBI performance of the proposed approach at various noise levels on 300 real carotid artery ultrasound images. Performance indicators show that the proposed approach outperforms other techniques at all mentioned noise levels which validate the robustness hypothesis of the proposed approach. In addition to this, the temporal comparison also represents that the proposed technique requires low computation time at reduced feature set.

Intelligent decision system is an important phase in medical image analysis. In this research work, we have designed a decision system based on SVM and obtained significant high classification accuracy of 98.84 %. This high classification accuracy indicates that the proposed model has potential to be used for clinical evaluation of carotid artery plaque.

The usefulness of the proposed segmentation technique is shown in the form of classification accuracy. Classification accuracy based on the proposed RSC-US segmentation approach has also been compared with recent published techniques. Santhiyakumari et al. [37] have used MLBPNN for classification and reported 96 % classification accuracy at their dataset. Chaudhry et al. [7] have utilized KNN to classify the have reported 98.3 % classification accuracy. Hassan et al. [15] have utilized MLBPNN classifier and achieved 98.4 % classification accuracy at their dataset, Whereas using the proposed segmentation approach, classification accuracy of 98.84 % is obtained by SVM classifier. Results indicate that classification using the proposed technique segmentation outperform the other techniques and hence show the usefulness of the proposed RSC-US segmentation approach. From Table 4, it can be observed that SVM outperforms the other classification techniques.

The proposed technique efficacy encourages using RSC-US as secondary observer for identification of plaque in carotid artery. Further, in country like Pakistan, it can also be used in remote areas with less-experienced technicians for initial screening of plaque buildup in carotid artery based on the ultrasound imaging.

It is assumed that the segmentation has a high impact on classification. To validate this hypothesis, we have utilized various segmentation and classification techniques. It has been observed from Fig. 13 and Table 2 that KNN, MLBPNN, and SVM offer high classification accuracy based on the proposed segmentation technique. Based on the proposed approach segmentation, classification accuracy has been improved by a margin of 2.47–4.00 % which is significant achievement. Hence, the hypothesis of effect of segmentation on classification has also been validated that better segmentation offers high classification rate.

5 Conclusions

In this paper, a new technique used for early carotid artery plaque detection to prevent from cerebrovascular accidents has been proposed. For this purpose, a new hybrid segmentation and classification approach employing neuro-fuzzy classifier, EM, and GA has been employed to carotid artery ultrasound images. For training, initial targets have been selected by the user and processed by EM algorithm to find accurate class labels. Optimized features have been selected by GA (4 out of 9) hence, used for segmentation. Utilizing the selected features, NFC has been employed to generate FIS hence, used for segmentation. Obtained segmentation results of the proposed technique have been compared visually and quantitatively with FCM, *K*-means, and sFCMLSM approaches. Further, to ensure robustness, the proposed approach has been gauged by considering various intensities of Gaussian noise into the original carotid artery ultrasound images. The proposed segmentation approach outperforms the other techniques both visually and quantitatively and successfully extracted ROI even in the presence of noise.

IMT is an important measure for plaque diagnosis in carotid artery. It has been measured from segmented images and fed as input to SVM classifier for separation of normal and abnormal subjects. Effect of segmentation on classification has also been investigated and results indicate that the proposed segmentation technique-based classification performance improved by a margin of 2.47–4.00 % (see Fig. 12; Table 2). Statistical analysis shows that accurate segmentation has high impact on classification accuracy. SVM, MLBPNN, and KNN classifiers have been employed and classification results have been compared. By using the proposed segmentation technique, SVM offers 98.84 % classification accuracy. The effectiveness of the proposed RSC-US technique segmentation is evident from the high classification accuracy. This technique can be used as a second observer to the radiologists to check the presence of plaque in the carotid artery. In future, we intend to apply texture analysis in conjunction with advanced computational intelligence technique for the prediction of disease using carotid artery ultrasound images.

Acknowledgments This research work is supported by the Higher Education Commission of Pakistan under the indigenous Ph.D. scholarship program [17-5-4(Ps4-078)/HEC/Sch/2008/]. The images used and the technical support have been provided by the radiology department Shifa International Hospital, Islamabad. With the full permission and consent of Shifa International Hospital, we have been used these images for research purposes (via Ref# Shifa/ISB/MG/RD/753/). The authors would like to extend their thanks to Shifa International Hospital, Islamabad, for providing data and technical support to complete this research work.

Compliance with ethical standards

Conflict of interest There are no conflicts of interest that could inappropriately influence this work.

Ethical approval All procedures performed in studies involving human participants were in accordance with the ethical standards of the institutional and/or national research committee and with the 1964 Declaration of Helsinki and its later amendments or comparable ethical standards (via Hosptial Ref# Shifa/ISB/MG/RD/753/).

Informed consent Informed consent was obtained from all individual participants included in the study.

References

1. Abdel-Dayem AR, El-Sakka MR, Fenster A (2005) Watershed segmentation for carotid artery ultrasound images. In: The 3rd ACS/IEEE international conference on computer systems and applications, p 131
2. Afridi T, Khan A, Lee Y (2012) Mito-GSAAC: mitochondria prediction using genetic ensemble classifier and split amino acid composition. Amino Acids 42:1443–1454. doi:10.1007/s00726-011-0888-0
3. Anders U, Korn O (1999) Model selection in neural networks. Neural Netw 12:309–323
4. Ayache N, Cinquin P, Cohen I, Cohen L, Leitner F, Monga O (1996) Segmentation of complex three dimensional medical objects: a challenge and a requirement for computer-assisted surgery planning and performance. In: Computer Integrated Surgery Technolology and Clinical Applications, MIT Press, pp 59–74
5. Borman S (2009) The expectation maximization algorithm—a short tutorial. Unpublished paper (online). https://www.cs.utah.edu/~piyush/teaching/EM_algorithm.pdf
6. Caldairou B, Passat N, Habas PA, Studholme C, Rousseau F (2011) A non-local fuzzy segmentation method: application to brain MRI. Pattern Recognit 44:1916–1927
7. Chaudhry A, Hassan M, Khan A, Kim J, Tuan T (2012) Automatic segmentation and decision making of carotid artery ultrasound images. In: Lee S, Cho H, Yoon K-J, Lee J (eds) Intelligent autonomous systems 12, vol 194. Advances in intelligent systems and computing. Springer, Berlin, pp 185–196
8. Chaudhry A, Hassan M, Khan A, Kim JY, Tuan TA (2012) Image clustering using improved spatial fuzzy C-means. In: Paper presented at the proceedings of the 6th international conference on ubiquitous information management and communication, Kuala Lumpur, Malaysia
9. Chih-Chung C, Chih-Jen L (2011) LIBSVM: a library for support vector machines. ACM Trans Intell Syst Technol 2:1–27. doi:10.1145/1961189.1961199
10. Christodoulou CI, Pattichis CS, Pantziaris M, Nicolaides A (2003) Texture-based classification of atherosclerotic carotid plaques. IEEE Trans Med Imaging 22:902–912
11. Chuang K-S, Tzeng H-L, Chen S, Wu J, Chen T-J (2006) Fuzzy c-means clustering with spatial information for image segmentaion. Comput Med Imaging Graph 30:9–15
12. Cristianini N, Taylor JS (2000) An introduction to support vector machines and other kernel-based learning methods. Cambridge University Press, Cambridge

13. Davies DL, Bouldin DW (1979) A cluster separation measure. IEEE Trans Pattern Anal Mach Intell 1:224–227
14. Golemati S, Stoitsis J, Sifakis E, Balkizas T, Nikita KS (2007) Using the Hough transform to segment ultrasound images of longitudinal and transverse sections of the carotid artery. Ultrasound Med Biol 33:1918–1932
15. Hassan M, Chaudhry A, Khan A, Kim JY (2012) Carotid artery image segmentation using modified spatial fuzzy c-means and ensemble clustering. Comput Methods Programs Biomed. doi:10.1016/j.cmpb.2012.1008.1011
16. Hayat M, Khan A, Yeasin M (2012) Prediction of membrane proteins using split amino acid and ensemble classification. Amino Acids 42:2447–2460. doi:10.1007/s00726-011-1053-5
17. Holmes G, Donkin A, Witten IH (1994) WEKA: a machine learning workbench. In: Proceedings of the second Australian and New Zealand conference on intelligent information systems, 29 November–2 December, pp 357–361
18. Iscan Z, Yüksel A, Dokur Z, Korürek M, Ölmez T (2009) Medical image segmentation with transform and moment based features and incremental supervised neural network. Digit Signal Proc 19:890–901
19. Kamel M, Campilho A, Abdel-Dayem A, El-Sakka M (2007) Fuzzy C-means clustering for segmenting carotid artery ultrasound images. In: Hutchison D, Kanade T, Kittler J, Kleinberg JM, Mattern F, Mitchell JC, Naor M, Pandu Rangan C, Steffen B, Terzopoulos D, Tygar D, Weikum G (eds) Image analysis and recognition, vol 4633. Lecture notes in computer science. Springer, Heidelberg, pp 935–948
20. Kamel M, Campilho A, Abdel-Dayem AR, El-Sakka MR (2005) Carotid artery ultrasound image segmentation using fuzzy region growing. In: Hutchison D, Kanade T, Kittler J, Kleinberg JM, Mattern F, Mitchell JC, Naor M, Pandu Rangan C, Steffen B, Terzopoulos D, Tygar D, Weikum G (eds) Image analysis and recognition, vol 3656. Lecture Notes in Computer Science. Springer, Berlin, pp 869–878
21. Karimi N, Samavi S, Shirani S, Behnamfar P (2010) Segmentation of DNA microarray images using an adaptive graph-based method. IET Image Process 4:19–27
22. Khan A, Siddiqa A, Munib S, Malik SA (2014) A recent survey of reversible watermarking techniques. Inf Sci 279:251–272. doi:10.1016/j.ins.2014.03.118
23. Li BN, Chui CK, Chang S, Ong SH (2011) Integrating spatial fuzzy clustering with level set methods for automated medical image segmentation. Comput Biol Med 41:1–10
24. Li W, Ogunbona P, deSilva C, Attikiouzel Y (2011) Semi-supervised maximum a posteriori probability segmentation of brain tissues from dual-echo magnetic resonance scans using incomplete training data. IET Image Process 5:222–232
25. Loizou C (2014) A review of ultrasound common carotid artery image and video segmentation techniques. Med Biol Eng Comput 52:1073–1093. doi:10.1007/s11517-014-1203-5
26. Loizou CP, Pattichis CS, Pantziaris M, Nicolaides A (2007) An integrated system for the segmentation of atherosclerotic carotid plaque. IEEE Trans Inf Technol Biomed 11:661–667
27. Vasantha M, Dr V, Bharathi Sunniah, Dhamodharan T (2010) Medical image features, extraction, selection and classification. Int J Eng Sci Technol 2:2071–2076
28. Mahmoud MS, Khalid HM (2013) Expectation maximization approach to data-based fault diagnostics. Inf Sci 235:80–96
29. Mao F, Gill J, Downey D, Fenster A (2000) Segmentation of carotid artery in ultrasound images. In: Proceedings of the 22nd annual international conference of the IEEE engineering in medicine and biology society, pp 1734–1737
30. Menchon-Lara R-M, Bastida-Jumilla M-C, Morales-Sánchez J, Sancho-Gómez J-L (2014) Automatic detection of the intima-media thickness in ultrasound images of the common carotid artery using neural networks. Med Biol Eng Comput 52:169–181. doi:10.1007/s11517-013-1128-4
31. Minghao P, Heon Gyu L, Couchol P, Keun Ho R (2010) A data mining approach for dyslipidemia disease prediction using carotid arterial feature vectors. In: IEEE 2nd international conference on computer engineering and technology (ICCET), Chengdu, April 16–18, pp V2-171–V172-175
32. Mitra S, Basak J (2001) FRBF: a fuzzy radial basis function network. Neural Comput Appl 10:244–252
33. Murphy SL, Xu J, Kochanek KD (2013) National vital statistics report. National Center for Health Statistics, Hyattsville
34. Ovchinnikov S (1991) Similarity relations, fuzzy partitions and fuzzy ordering. Fuzzy Sets Syst 40:107–126
35. Park SH, Goo JM, Jo C-H (2004) Receiver operating characteristic (ROC) curve: practical review for radiologists. Korean J Radiol 5(1):11–18
36. Rocha R, Al Campilho, Silva J, Azevedo E, Santos R (2011) Segmentation of ultrasound images of the carotid using RANSAC and cubic splines. Comput Methods Programs Biomed 101:94–106
37. Santhiyakumari N, Rajendran P, Madheswaran M (2011) Medical decision-making system of ultrasound carotid artery intima-media thickness using neural networks. J Digit Imaging 24:1112–1125
38. Smith SM, Fox PT, Miller KL, Glahn DC, Fox PM, Mackay CE, Filippini N, Watkins KE, Toro R, Laird AR, Beckmann CF (2009) Correspondence of the brain's functional architecture during activation and rest. Proc Natl Acad Sci 106:13040–13045. doi:10.1073/pnas.0905267106
39. Svozil D, Vr Kvasnicka, Pospichal JÃ (1997) Introduction to multi-layer feed-forward neural networks. Chemom Intell Lab Syst 39:43–62
40. Tan J, Lim Joon D, Fitt G, Wada M, Lim Joon M, Mercuri A, Marr M, Chao M, Khoo V (2010) The utility of multimodality imaging with CT and MRI in defining rectal tumour volumes for radiotherapy treatment planning: a pilot study. J Med Imaging Radiat Oncol 54:562–568
41. Velakoulis D, Wood SJ, Wong MH (2006) Hippocampal and amygdala volumes according to psychosis stage and diagnosis: a magnetic resonance imaging study of chronic schizophrenia, first-episode psychosis, and ultra-high-risk individuals. Arch Gen Psychiatry 63:139–149
42. Xu X, Zhou Y, Cheng X, Song E, Li G (2012) Ultrasound intima-media segmentation using Hough transform and dual snake model. Comput Med Imaging Graph 36:248–258. doi:10.1016/j.compmedimag.2011.06.007
43. Zadeh LA (1996) Fuzzy sets and their application to pattern classification and clustering analysis. In: George JK, Bo Y (eds) Fuzzy sets, fuzzy logic, and fuzzy systems. World Scientific, Singapore, pp 355–393

Asmatullah Chaudhry received his M.Sc. degree in Physics from Islamia University Bahawalpur, Pakistan, in 1993 and his M.S. degree in Nuclear Engineering from Pakistan Institute of Engineering and Applied Sciences (PIEAS), Islamabad, Pakistan, in 1998. He received his M.S. and Ph.D. degrees in Computer Systems Engineering from GIK Institute, Topi, Pakistan, in 2003 and 2007, respectively. He has more than 13 years of research experience and is working as Principal Scientist in HRD Division at PINSTECH. His research areas include image processing, pattern recognition, and machine learning.

Mehdi Hassan received his M.Sc. degree in Computer Science from Gomal University, D.I. Khan, in 2004. He received his M.S. degree in Computer System Engineering from GIK Institute, Topi, Pakistan, in 2010 and Ph.D. degree from Pakistan Institute of Engineering and Applied Sciences (PIEAS), Islamabad, Pakistan, in 2015, respectively. His research interests are biomedical image processing and analysis, pattern recognition, machine learning, data mining and neural networks. Currently he is working as Assistant Professor at Department of Computer Science and Engineering, Air University Islamabad, Pakistan.

Asifullah Khan received his M.Sc. degree in Physics from University of Peshawar, Pakistan, in 1996 and his M.S. degree in Nuclear Engineering from PIEAS, Islamabad, Pakistan, in 1998. He received his M.S. and Ph.D. degrees in Computer Systems Engineering from GIK Institute, Topi, Pakistan, in 2003 and 2006, respectively. He has carried out 2-years Post-Doc Research at Signal and Image Processing Lab, Department of Mechatronics, GIST, South Korea. He has more than 13 years of research experience and is working as Associate Professor in DCIS at PIEAS. His research areas include digital watermarking, pattern recognition, image processing, evolutionary algorithms, bioinformatics, machine learning, and computational materials science.